JOURNAL OF PHYSICAL ORGANIC CHEMISTRY, VOL. 10, 435–444 (1997)

SUPRAMOLECULAR DONOR–ACCEPTOR COMPLEXES OF DICHLOROFLUORESCEIN AND *cis*- AND *trans*-4,4′-(*N*,*N*′-DIMETHYLPYRIDINIUM)ETHYLENE

ITAMAR WILLNER,[1]* SHARON MARX-TIBBON,[1] SHMUEL COHEN,[1] YOAV EICHEN[2] AND MENACHEM KAFTORI[2]

[1] *Institute of Chemistry and Farkas Center for Light-Induced Processes, The Hebrew University of Jerusalem, Jerusalem 91904, Israel*
[2] *Department of Chemistry, The Technion Institute of Technology, Haifa 32000, Israel*

***trans*-4,4′(*N*,*N*′-Dimethylpyridinium)ethylene [*trans*-(1)] and *cis*-4,4′(*N*,*N*′-dimethylpyridinium)ethylene [*cis*-1] form with 2,7-dichlorofluorescein [DCF^{2-}, (2)] donor–acceptor complexes of 1:1 stoichiometry [*K*(*trans*-1) = 14 000 M^{-1} and *K*(*cis*-1) = 300 M^{-1} in water]. The lower affinity of *cis*-1 to form the donor–acceptor complex with DCF^{2-}, (2), is attributed to the non-planar structure of *cis*-1 (tilt-angle between the pyridinium rings = 26°). The solid-state structure of the complex between DCF^{2-} and *trans*-1 indicates alternate stacking of donor and acceptor units with an inter-layer spacing of 3·4 Å. Solubilization of the crystalline DCF^{2-} and *trans*-1 complex in water or dimethylformamide (DMF) results in the initial formation of a non-symmetric complex where a *trans*-1 unit is inter-layered between two DCF^{2-} components, and a second *trans*-1 unit is located externally to the supramolecular assembly and participates in charge neutralization [$(DCF^{2-})_2 \cdots$*trans*-1/*trans*-1]. The primary non-symmetrical complex is thermally transformed to a themodynamically stable symmetric complex where the DCF^{2-} and *trans*-1 form a sandwich-type layered assembly [$DCF^{2-} \cdots$*trans*-1]. The structural features of the complexes were characterized by ^{1}H-NMR spectroscopy. The kinetics of the transformation of the [$(DCF^{2-})_2 \cdots$*trans*-1/trans-1] complex to the [$DCF^{2-} \cdots$*trans*-1] assembly was spectroscopically characterized in DMF ($k = 0{\cdot}22\ s^{-1}$ at 322 K; E_a = 20 kcal mol^{-1}). © 1997 by John Wiley & Sons, Ltd.**

J. Phys. Org. Chem. **10**, 435–444 (1997) No. of Figures: 10 No. of Tables: 1 No. of References: 20

Keywords: supramolecular donor–acceptor complexes; dichlorofluorescein; *cis*- and *trans*-4,4′(*N*,*N*′-dimethylpyridinium)ethylene

Received 25 November 1996; revised January 1997; accepted 29 January 1997

INTRODUCTION

Attractive interactions between π-systems control the formation of diverse molecular complexes. Stabilization of the double helical structure of DNA,[1] intercalation of drugs into DNA,[2,3] stacking of aromatic molecules in the solid state,[4] formation of host–guest complexes[5,6] and aggregation of organic dyes[7] or porphyrins originate from intermolecular $\pi-\pi$ interactions. Theoretical studies addressed the significance of π-interactions in controlling the orientation and the structure of π-stacked systems.[8,9] Electron donor–acceptor interactions provide another route to stabilize supramolecular complexes.[10] Selective molecular complexation in biological systems,[11] formation of supramolecular host–guest complexes[12] and rigidified non-covalently linked assemblies[13,14] were attributed to intermolecular stabilization of the assemblies by donor–acceptor interactions. Xanthene dyes form intermolecular complexes with *N*,*N*′-dialkyl-4,4′-bipyridinium salts. The complexes are stabilized by donor–acceptor interactions and cooperatively by electrostatic attractive forces.[15,16] It was shown that the xanthene dye–*N*,*N*′-dialkyl-4,4′-bipyridinium complexes in the solid state crystallize in diverse configurations.[15] Linearly stacked donor–acceptor complexes with alternate overlap positioning of the xanthene dye donor and the bipyridinium acceptor units were observed, i.e. the complex between eosin and *N*,*N*′-dimethyl-4,4′-bipyridinium. An alternative structure included the stacked intercalation of one acceptor unit between two xanthene dye electron donor components, and external neutralization of the complex by an additional bipyridinium unit, i.e. the complex between eosin and *N*,*N*′-dibenzyl-4,4′-bipyridinium.[15] The formation of supramolecular xanthene dye—bipyridinium complexes of variable stoichiometries and structures was also observed in solutions.[15] Transformations between kinetically favored structures and thermodynamically stable supramolecular assemblies have been reported.[15] For example, eosin and *N*,*N*′-dimethyl-4,4′- bipyridinium forms in DMF a kinet-

* *Correspondence to:* I. Willner.

 CCC 0894–3230/97/060435–10 $17.50

ically favored 1:1 eosin complex that is thermally transformed into a complex where one bipyridinium unit is inter-layered between two eosin components, and a second bipyridinium is located externally to the intermolecuar assembly and acts for charge neutralization.[15]

Donor–acceptor complexes between xanthene dyes and bipyridinium electron acceptors have recently been used to tailor photochemical supramolecular switches[17] and molecular optoelectronic devices.[18] For example, a bipyridinium–azobenzene diad acted as photoactive electron acceptor to trigger by light the formation of the supramolecular complex with eosin and its dissociation.[17] Photoisomerization of the diad to the *cis*-azobenzene state stimulates the formation of the donor–aceptor complex with eosin, where photoisomerization of the diad to the bipyridinium–*trans*-azobenzene state effects the dissociation of the complex. By cyclic photoisomerization of the diad between the two states, reversible light-induced formation and dissociation of the complex were observed and transduced by the chromophore spectrum in the complexed and free states. The eosin donor was also assembled as a monolayer on an Au electrode.[18] Formation and dissociation of the complex at the monolayer electrode, in the two isomer states of the bipyridinium–azobenzene, were transduced electrochemically utilizing the electroactivity of the bipyridinium unit.[18] Alternatively, microgravimetric, quartz crystal microbalance, piezoelectric analysis of the formation and dissociation of the complex at the monolayer interface was employed as an electronic transduction means of the optical signals recorded by the photoactive diad.[18]

Bifunctional, conjugated bispyridinium salts are expected to exhibit built-in isomeric states. These structural isomers should exhibit different affinities for xanthene dye donors. Thus, by the introduction of functional units that are capable of triggering interconversion between the isomers, new electron acceptors for the assembly of molecular switches could be envisaged. Here we report on the supramolecular donor–acceptor complexes beween *trans*-4,4′(*N*,*N*′-dimethylpyridinium)ethylene (*trans* − **1**) and *cis*-4,4′-(*N*,*N*′-dimethylpyridinium)ethylene (*cis* − **1**), with 2,7-dichlorofluorescein [DCF^{2-}, (**2**)]. We find that the two isomeric states exhibit substantially different affinities for the dichlorofluorescein electron donor. The formation of the intermolecular complex between DCF^{2-} and *cis*-**1** is inhibited owing to perturbation of the planarity of the π-system. We also present the solid-state structure and the solution features of the complexes formed between DCF^{2-} and *trans*-**1**.

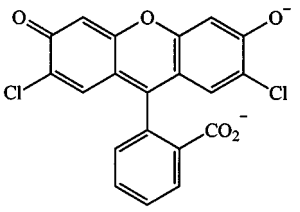

(2)

EXPERIMENTAL

Instruments. Absorption spectra were recorded on a Uvikon 860 spectrophotometer (Kontron) equipped with a thermostated cell. Emission spectra were recorded on a Uvikon SFM 25 fluoremeter (Kontron). NMR spectra were recorded on a DRX 400 (400·13 MHz) or WP200 (200 MHz) spectrometer (Bruker).

For x-ray crystal structure analysis, data were measured on a PW1100/20 four-circle diffractometer (Philips). Mo Kα radiation ($\lambda = 0{\cdot}71069$ Å) was used for the *cis*-**1** compound, and on an ENRAF-Nonius CAD-4 automatic diffractometer Cu Kα radiation ($\lambda = 1{\cdot}54178$ Å) was used for the [DCF^{2-}–*trans*-**1**] complex. The unit cell dimensions were obtained by a least-squares fit of 24 centered reflections in the range $12 \leqslant \theta \leqslant 15°$ for *cis*-**1** and $23 \leqslant \theta \leqslant 28°$ for [DCF^{2-}–*trans*-**1**]. Intensity data were collected using the $\omega - 2\theta$ technique to a maximum $2\theta = 46°$ for *cis*-**1** and 120° for [DCF^{2-}–*trans*-**1**]. The scan width, $\Delta\omega$, for each reflection was $1{\cdot}00 + 0{\cdot}35 \tan\theta$ with a scan speed of $3{\cdot}0°$ min^{-1} and $0{\cdot}80 + 0{\cdot}15 \tan\theta$ with a scan speed of $8{\cdot}24°$ min^{-1} for *cis*-**1** and for [DCF^{2-}–*trans*-**1**], respectively. Intensities were corrected for Lorentz and polarization effects. All non-hydrogen atoms were found by using the results of the SHELXS-86 direct method analysis.[19] After several cycles of refinements the positions of the hydrogen atoms were calculated, and added to the refinement process. Refinement proceeded to convergence by minimizing the function $\Sigma w(|F_o| - |F_c|)^2$. A final difference Fourier synthesis map showed several peaks less than $1{\cdot}0$ e Å^{-3} (*cis*-**1**) and $0{\cdot}4$ e Å^{-3} ([DCF^{2-}–*trans*-**1**]) scattered about the unit cell without a significant feature. The discrepancy indices, $R = \Sigma||F_o| - |F_c||/\Sigma|F_o|$ and $R_w = [\Sigma w(|F_o| - |F_c|)^2/\Sigma w|F_o|^2]^{1/2}$ are 0·033 and 0·048 for *cis*-**1** and 0·055 and 0·083 for [DCF^{2-}–*trans*-**1**].

Single crystals were obtained by slow evaporation of saturated solutions of the complex and *cis*-**1**.

Materials. *trans*-4,4′-(*N*,*N*′-Dimethylpyridinium)ethylene (*trans*-**1**) was prepared (Scheme 1) by adding 2·32 g (16·4 mmol) of methyl iodide dropwise to a refluxing solution of 1·5 g (5·2 mmol) of *trans*-1,2-bis(4-pyridyl)-ethylene (Aldrich) in 10 ml of acetonitrile. The solution was heated for 2 h until orange crystals appeared. The crystals were recrystallized from ethanol. ^{1}H NMR (D_2O, 400·13 MHz): $\delta = 8{\cdot}8$ ppm (d, 4H, $J = 6{\cdot}8$ Hz), 8·25 (d, 4H, $J = 6{\cdot}8$ Hz), 7·89 (s, 2H), 4·4 (s, 6H).

cis-4,4′(*N*,*N*′-dimethylpyridinium)ethylene (*cis*-**1**) was prepared (Scheme 1) according to the literature,[20] by the benzil-sensitized photoisomerization of *trans*-1,2-bis(4-pyridyl)ethylene and chromatographic separation over alumina, using 5% benzene in hexane as eluent, followed by quaternization of the product with methyl iodide as described before. ^{1}H NMR (D_2O, 200 MHz): $\delta = 8{\cdot}3$ ppm (m, 7H), 7·14 (s, 2H), 4·36 (s, 6H).

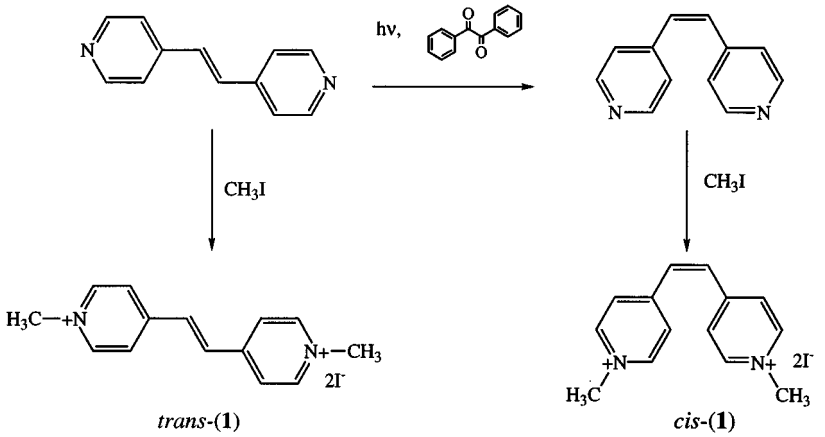

Scheme 1. Synthetic route for the preparation of *trans*-**1** and *cis*-**1**.

2,7-Dichlorofluorescein was purchased from Aldrich and used without further purification. All other chemicals were obtained from Sigma and Aldrich and were used without further purification.

RESULTS AND DISCUSSION

Figure 1 shows the x-ray stucture of *cis*-**1**. The pyridinium units are not coplanar with the ethylene bond and their planes are tilted one to another by 26°. This tilting angle is attributed to steric *peri* repulsive interactions between H-atoms of the two pyridinium rings that distort the π-system from planarity. On the other hand, *trans*-**1** is a planar molecule and the dihedral angle between the pyridinium units is 180°. The donor–acceptor complexes between DCF^{2-} (**2**) and *trans*- and *cis*-**1** were characterized in aqueous solution. Figure 2(A) shows the spectral changes of DCF^{2-} upon addition of *trans*-**1**. The absorbance maximum of DCF^{2-} is red-shifted. The observation of a single isosbestic point upon addition of *trans*-**1** indicates the formation of a single type of supramolecular complex between DCF^{2-} and *trans*-**1**. The spectral changes of DCF^{2-} upon addition of different concentrations of *trans*-**1** were used to calculate the complex association constant, K_a [equations (1) and (2)] according to the Benesi–Hildebrand relation [equation (3)], where $[A]^0$ and $[D]^0$ are the analytical concentrations of the donor and acceptor, respectively, ΔOD is the absorbance change at a certain wavelength (in the specific example $\lambda = 519$ nm) and $\Delta\epsilon$ is the difference between the molar extinction coefficient of the free donor and the associated donor at this wavelength.

$$DCF^{2-} + A \overset{K_a}{\rightleftharpoons} [DCF^{2-} \cdots A] \quad [A = \textit{trans}\text{- or } \textit{cis}\text{-}\mathbf{1}) \quad (1)$$

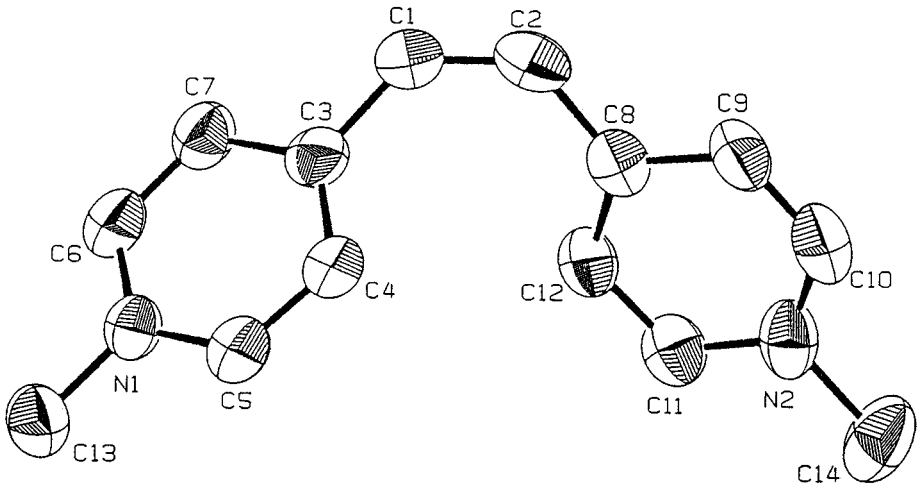

Figure 1. X-ray structure of *cis*-**1**.

$$K_a = \frac{[DCF^{2-} \cdots A]}{[DCF^{2-}]_f[A]_f} \quad (2)$$

$$\frac{[A]^0[DCF]^0}{\Delta OD} = \frac{([A]^0 + [DCF^{2-}]^0)}{\Delta\epsilon} + \frac{1}{K_a\Delta\epsilon} \quad (3)$$

Figure 2(B) shows the analysis of the observed spectral changes of DCF^{2-} upon addition of *trans*-**1** according to equation (3). A linear relationship is obtained and the derived association constant for the intermolecular complex, $[DCF^{2-} \cdots$*trans*-**1**$]$, corresponds to $K_a = 14000 \pm 600\ M^{-1}$. The Benesi–Hildebrand equation assumes the formation of a 1:1 complex between the molecular components. The linear relationship obtained by analysis of the spectral changes, ΔOD, at different *trans*-**1** concentrations [Figure 2(B)] thus supports the formation of a 1:1 supramolecular donor–acceptor complex between the components. The association constant of *cis*-**1** to DCF^{2-} was similarly characterized. The latter acceptor forms a substantially less stable complex. The derived association constant for the complex, $[DCF^{2-} \cdots$*cis*-**1**$]$, is $K_a = 300 \pm 100\ M^{-1}$. This difference is attributed to the nonplanar configuration of *cis*-**1**. For effective stabilization of intermolecular donor–acceptor complexes, the donor and acceptor units should be parallel one to the other to achieve effective $\pi-\pi$ overlap. In addition to the $\pi-\pi$ overlap, the donor–acceptor complexes between xanthene dyes and bipyridinium salts are further stabilized by attractive electrostatic interactions. The distorted π-system of *cis*-**1** presumably perturbs the $\pi-\pi$ overlap and the electrostatic attractive interactions between the donor (DCF^{2-}) and the acceptor unit (*cis*-**1**), leading to the lower association constant.

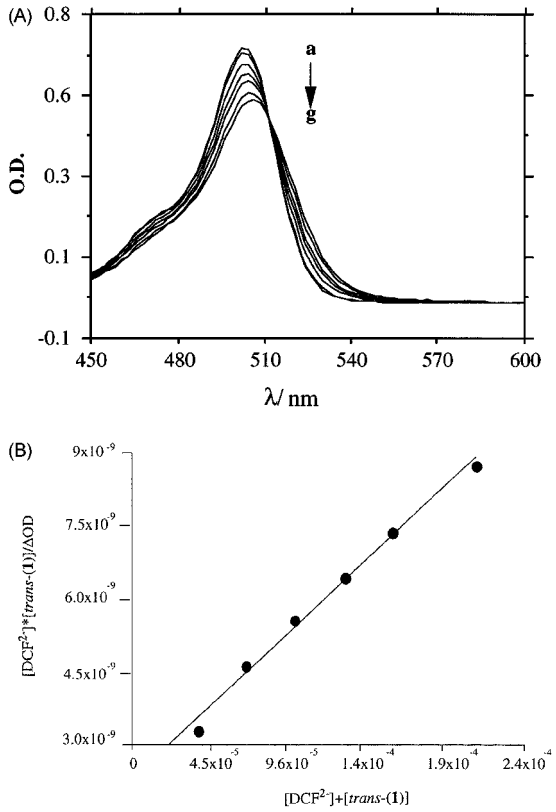

Figure 2. (A) Absorption spectra of DCF^{2-} (**2**) (8×10^{-6} M) upon addition of *trans*-**1**: (a) 0; (b) 3×10^{-5}; (c) 6×10^{-5}; (d) 9×10^{-5}; (e) $1{\cdot}2\times10^{-4}$; (f) $1{\cdot}5\times10^{-4}$; (g) 2×10^{-4} M. Spectra recorded at 25 °C. (B) Benesi–Hildebrand analysis of the spectral changes, ΔOD of DCF^{2-}, upon additon of *trans*-**1**.

The association constants between DCF^{2-} and *trans*-**1** and *cis*-**1** can be further characterized by analyzing the fluorescence quenching of the chromophore in the presence of the electron acceptors. Figure 3(A) shows the fluorescence quenching spectra of DCF^{2-} at different concentrations of *trans*-**1**. Figure 3(B) (line a) shows the analysis of the fluorescence quenching according to the Stern–Volmer equation [equation (4)]. The derived Stern–Volmer constant corresponds to K_{sv}(*trans*-**1**)$= 13\,750 \pm 300\ M^{-1}$. The fluorescence quenching of DCF^{2-} by *cis*-**1** is substantially less effective. Figure 3(B) (line b) shows the Stern–Volmer plot for the fluorescence quenching of DCF^{2-} by *cis*-**1**. The derived Stern–Volmer constant K_{sv}(*cis*-**1**)$= 340 \pm 80\ M^{-1}$. Assuming that the formation of the supramolecular complexes between DCF^{2-} and *trans*- or *cis*-**1** results in static quenching of the chromophore, the experimental Stern–Volmer constants are essentially the association constants of the respective complexes. Static quenching of DCF^{2-} by the electron acceptor implies that the observed fluorescence upon addition of the electron acceptor originates from the free chromophore present in equilibrium ($I \propto [DCF^{2-}]_f$). Thus, equation (2) can be reorganized in terms of equation (5), which essentially coincides with the Stern–Volmer relation. Thus, we realize that the association constants of the complexes $[DCF^{2-} \cdots$*trans*-**1**$]$ and $[DCF^{2-} \cdots$*cis*-**1**$]$ derived by the fluorescence quenching experiments are in excellent agreement with the values obtained by the spectral analyses of the chromophore.

$$\frac{I_0}{I} = 1 + K_{SV}[A] \quad (4)$$

$$K_a[A]_f = \frac{[DCF^{2-} \cdots A]}{[DCF^{2-}]_f} = \frac{[DCF^{2-}]_0 - [DCF^{2-}]_f}{[DCF^{2-}]_f} = \frac{I_0 - I}{I} \quad (5)$$

The structure of the intermolecular complex between DCF^{2-} and *trans*-**1** was elucidated in the solid state and in solution. Figure 4 shows the x-ray structure of the complex $[DCF^{2-} \cdots$*trans*-**1**$]$. Stacks that include alternate layers of DCF^{2-} and *trans*-**1** are observed. The *trans*-**1** electron acceptor in the complex structure is planar. The inter-layer

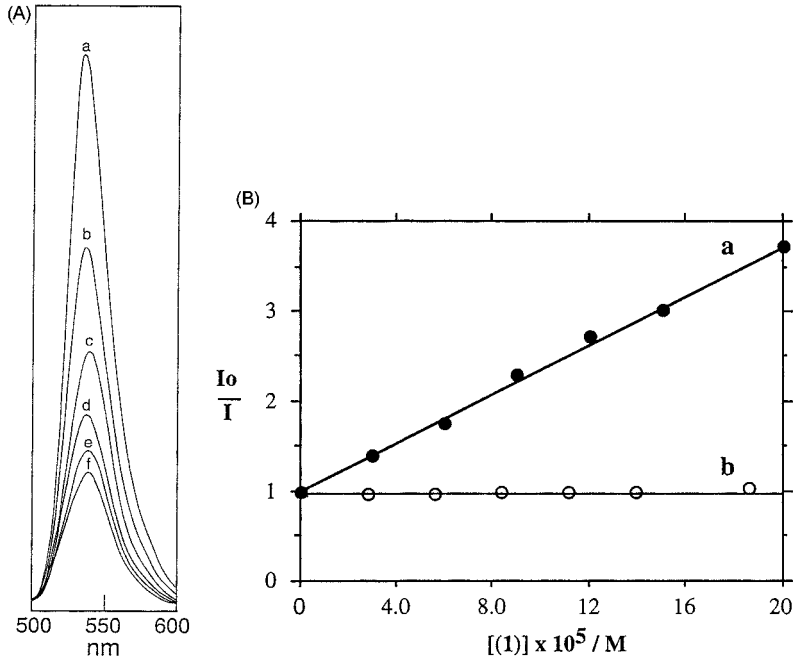

Figure 3. (A) Fluorescence quenching spectra of DCF^{2-} (**2**) (8×10^{-6} M) upon addition of *trans*-**1**: (a) 0; (b) $1{\cdot}3\times10^{-4}$; (c) $2{\cdot}06\times10^{-5}$; (d) $3{\cdot}09\times10^{-5}$; (e) $4{\cdot}12\times10^{-5}$; (f) $5{\cdot}10\times10^{-5}$ M. For all experiments λ_{exc} = 500 nm. (B) Stern–Volmer analysis of the fluorescence quenching of DCF^{2-} by (a) *trans*-**1** and (b) *cis*-**1**.

spacing between the electron acceptor and adjacent DCF^{2-} layers is 3·4 Å. This is a typical value for intermolecular donor–acceptor complexes. A closely related spacing (3·4 Å) was observed for other complexes resulting from

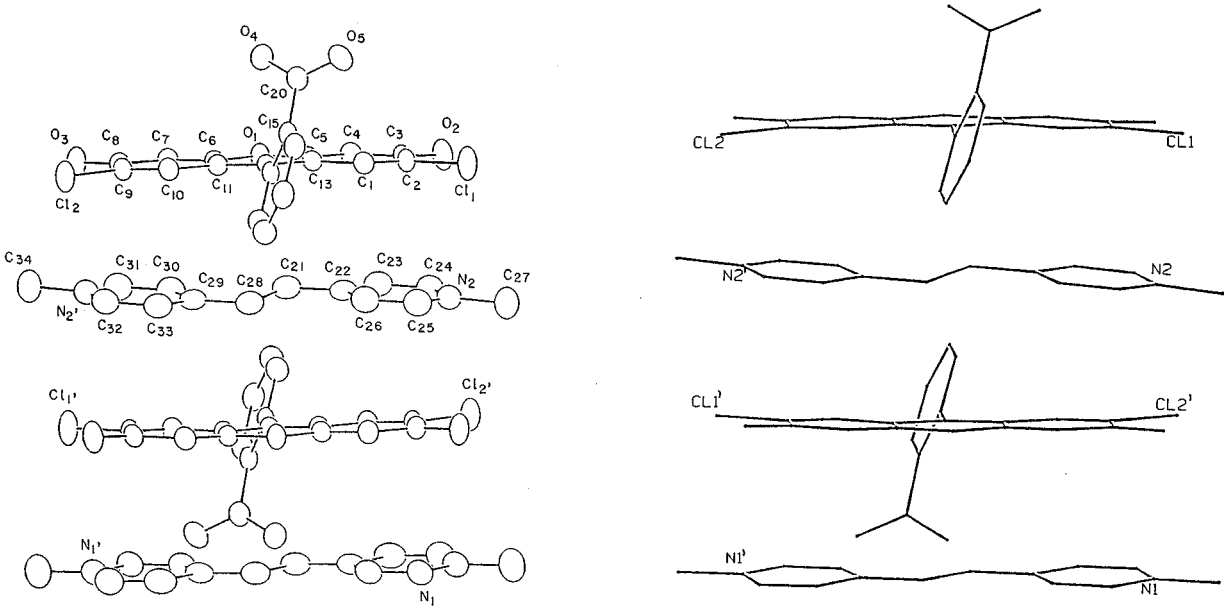

Figure 4. X-ray structure of the [DCF^{2-}-*trans*-**1**] complex.

Table 1. Important bond angles and bond lengths of the crystal of [DCF^{2-} · · ·*trans*-**1**]

Atoms	Bond length (Å)	Bond angle (°)
C_{12}—C_{14}	1·497	
C_2—Cl_1	1·733	
C_3—O_2	1·268	
C_{15}—C_{20}	1·506	
N_1—C_{27}	1·480	
C_{21}—C_{22}	1·464	
O_2—C_3—C_4		123·2
Cl_1—C_2—C_3		123·2
C_{14}—C_{15}—C_{20}		122·1
C_{12}—C_{14}—C_{15}		122·4
C_{27}—N_1—C_{25}		119·8
C_{24}—N_1—C_{25}		120·0

xanthene dyes and bipyridinium electron acceptors.[15] Important bond angles and bond lengths of the supramolecular complex [DCF^{2-} · · ·*trans*-**1**] are summarized in Table 1. The crystal does not include the initial counterions (I^- for *trans*-**1** and $2Na^+$ for DCF^{2-}), indicating that the two complex components self-neutralize in the crystal. The carboxyphenyl ring of DCF^{2-} is tilted towards one end of *trans*-**1** and the tilting direction is opposite from one DCF^{2-} to the other. This tilting is attributed to the neutralization of one of the pyridinium rings by the carboxylate anion of the carboxyphenyl residue. The other pyridinium ring is neutralized by the phenolate anion which is part of the planar tricyclic ring layer of DCF^{2-}. Thus, the x-ray structure of [DCF^{2-} · · ·*trans*-**1**] reveals that the donor–acceptor units are arranged in an optimized configuration to attain maximum interlayer π–π overlap and effective intermolecular charge neutralization. Our attemps to crystallize the complex [DCF^{2-} · · ·*cis*-**1**] failed. Realizing the non-planar structure of *cis*-**1** (see above), the formation of a layered donor–acceptor structure with short inter-spacing of the π-systems is prohibited. This could explain the low association constant for [DCF^{2-} · · ·*cis*-**1**] and the failure to obtain single crystals.

Insight into the structural features of the complex formed between DCF^{2-} and *trans*-**1** in water was obtained by ^{1}H NMR spectroscopy. Single crystals of [DCF^{2-} · · ·*trans*-**1**] were dissolved in D_2O. Under these conditions, the solubilized complex is stabilized only by intermolecular interaction, without the involvement of counterions. Figure 5(A) shows the resulting ^{1}H NMR spectrum of the solution. Interestingly, in the region 7·98–8·9 ppm *two* pairs of AB spectra are observed, characteristic of protons H_a and H_b of *trans*-**1**. One pair appears at δ=8·83 and 7·98 ppm, whereas the second pair is observed at δ=8·23 and 8·62 ppm. The appearance of two distinct AB systems was further confirmed by ^{1}H-COSY experiments. Note that the methyl groups associated with the pyridinium units also appear as *two* singlets at δ=4·3 and 4·4 ppm. The chemical shifts observed in the region 7·2–7·85 ppm are characteristic of the DCF^{2-} component of the complex. Integration of the respective bands reveal that the ratio between the *two* bipyridinium sets of chemical shifts and the DCF^{2-} chemical shifts is 1:1. This implies that the complex that is formed upon dissolution of the single crystal of [DCF^{2-} · · ·*trans*-**1**] in water exhibits a structure that includes two DCF^{2-} units and two *trans*-**1** units. The two DCF^{2-} components are symmetric relative to one of the *trans*-**1** electron acceptor sites, whereas the second *trans*-**1** unit is located in a non-symmetric different position relative to the assembly. Scheme 2, structure A, outlines schematically a proposed configuration of the complex in solution. One *trans*-**1** unit is inter-layered between two symmetrical DCF^{2-} units, whereas the second *trans*-**1** unit is located externally to the intermolecular [(DCF^{2-}) · · *trans*-**1**] cluster, and participates in the electrical neutralization of the assembly. In fact, a closely related structure was documented in the solid state for a complex between eosin and *N*,*N*′-dibenzyl-4,4′-bipyridinium.[15] Heating of the complex solution at 355 K for 3 h results in the ^{1}H NMR spectrum shown in Figure 5(B). The two sets of chemical shifts that correspond to *two* different *trans*-**1** components transform to a *single* AB set at δ=8·29 and 8·88 ppm. Also, only a *single* chemical shift for the methyl protons associated with the pyridinium units is observed at δ=4·35 ppm. The integration between the single *trans*-**1** chemical shifts and the DCF^{2-} chemical shifts indicates the intermolecular ratio of 1:1. This thermal transformation is irreversible and cooling of the sample does not alter the ^{1}H NMR spectrum. Thus, heating of the [(DCF^{2-})$_2$ · · ·*trans*-**1**/*trans*-**1**] complex results in a new complex of simple 1:1 stoichiometry between DCF^{2-} and *trans*-**1**. Scheme 2, structure B, outlines schematically the suggested structure of the resulting complex. A layered donor–acceptor complex of DCF^{2-} and *trans*-**1** is consistent with the experimental results. Again, this layered structure was observed in the solid state for various xanthene dyes and bipyridinium salts, i.e. the complex between eosin and *N*,*N*′-dibenzyl-4,4′-bipyridinium.[15] It should be noted that the stoichiometries of the kinetically favored [(DCF^{2-})$_2$ · · ·*trans*-**1**/trans-**1**] complex and of the thermally generated [DCF^{2-} · · ·*trans*-**1**] complex obey a general stoichiometry of 1:1. The association constants that were derived spectroscopically for the complex correspond to the kinetically favored assembly [(DCF^{2-})$_2$ · · ·*trans*-**1**/*trans*-**1**].

The association constants of xanthene dye–bipyridinium donor–acceptor complexes and their interconversion rates between variable stoichiometries depend on the solvent. The association constants between DCF^{2-} and *trans*- or *cis*-**1** were also spectroscopically characterized in dimethylformamide (DMF). The derived value for the complex between DCF^{2-} and *trans*-**1** corresponds to K_a=21 000 M^{-1} whereas the association constant for the intermolecular complex between DCF^{2-} and *cis*-**1** is K_a=5300 M^{-1}. Hence the affinities of the two isomers for DCF^{2-} differ substantially also in DMF. The complex between DCF^{2-} and *cis*-**1** is substantially weaker than the intermolecular complex between DCF^{2-} and *trans*-**1**. The

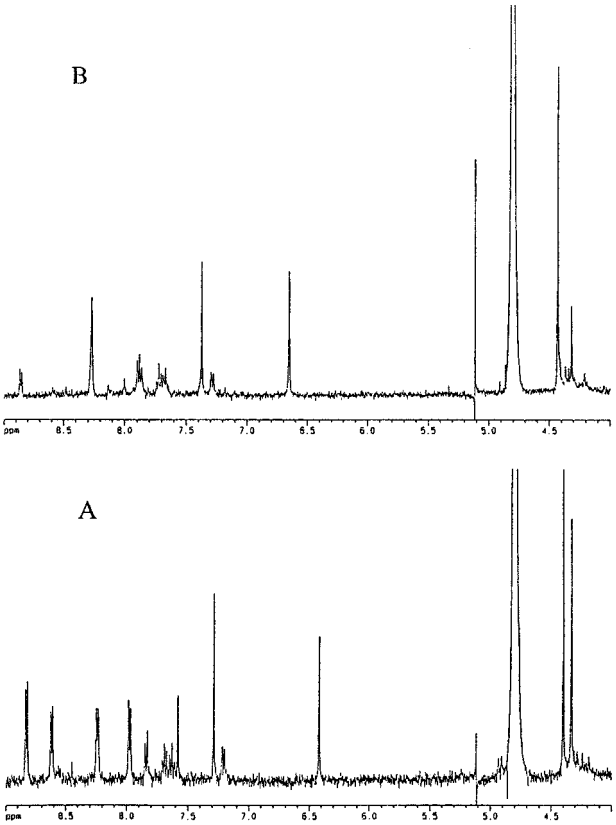

Figure 5. (A) ^{1}H NMR spectrum (D_2O) of an immediately dissolved [$DCF^{2-} \cdots$*trans*-**1**] complex. (B) ^{1}H NMR spectrum (D_2O) of the complex after heating the solution for 3 h at 355 K.

^{1}H NMR spectrum of the complex between DCF^{2-} and *trans*-**1** in DMF-d_7 similarly shows the transformation of the [$(DCF^{2-})_2 \cdots$*trans*-**1**/*trans*-**1**] complex to the symmetric [$DCF^{2-} \cdots$*trans*-**1**] (1:1) complex (Figure 6). Figure 6(A) shows the chemical shift region of the *trans*-**1** component upon dissolution of the precipitated [$DCF^{2-} \cdots$*trans*-**1**] complex. Two pairs of AB spectra are observed [Figure 6(A), (a)], one at 8·43 and 8·91 ppm and the other at 8·32 and 9·10 ppm. Note that the two pairs do not exhibit a 1:1 ratio. Heating the sample to 320 K for 10 min transforms the two AB pairs into a simple AB pattern that appears at 8·32 and 9·10 ppm. It should be noted that in order to dissolve the [$DCF^{2-} \cdots$*trans*-**1**] solid complex in DMF, slight heating was required. Thus, already upon dissolution of the complex, part of the [$(DCF^{2-})_2 \cdots$*trans*-**1**/*trans*-**1**] complex (giving rise to the two AB pairs) was thermally transformed to the symmetrical (1:1) supramolecular complex [$(DCF^{2-}) \cdots$*trans*-**1**]. The later complex exhibits a simple AB spectrum for the *trans*-**1** component that overlaps with one of the AB pairs of the kinetically produced complex. This gives rise to the unequal ratio of the two AB spectra of [$(DCF^{2-})_2 \ldots$ *trans*-**1**/*trans*-**1**] complex in the original solution. This explanation is further supported by following the methyl protons chemical shifts associated with the pyridinium rings of *trans*-**1** in the various complexes [Figure 6(B)]. Upon dissolution of the solid [$DCF^{2-} \cdots$*trans*-**1**] complex, two singlets of unequal ratio at δ=4·48 and 4·51 ppm are observed [Figure 6(A), (b)]. Upon heating the sample to 320 K for 90 min the methyl protons transform to a simple singlet centered at 4·52 ppm [Figure 6(B), (b)]. This confirms that the initial

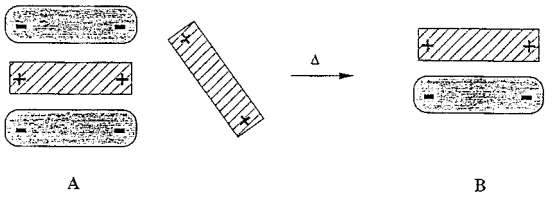

Scheme 2. Suggested configuration of the kinetically generated, non-symmetrical, [$(DCF^{2-})_2 \cdots$*trans*-**1**/*trans*-**1**] complex structure (A), and thermodynamically stable [$DCF^{2-} \cdots$*trans*-**1**] structure B, in water and DMF solutions.

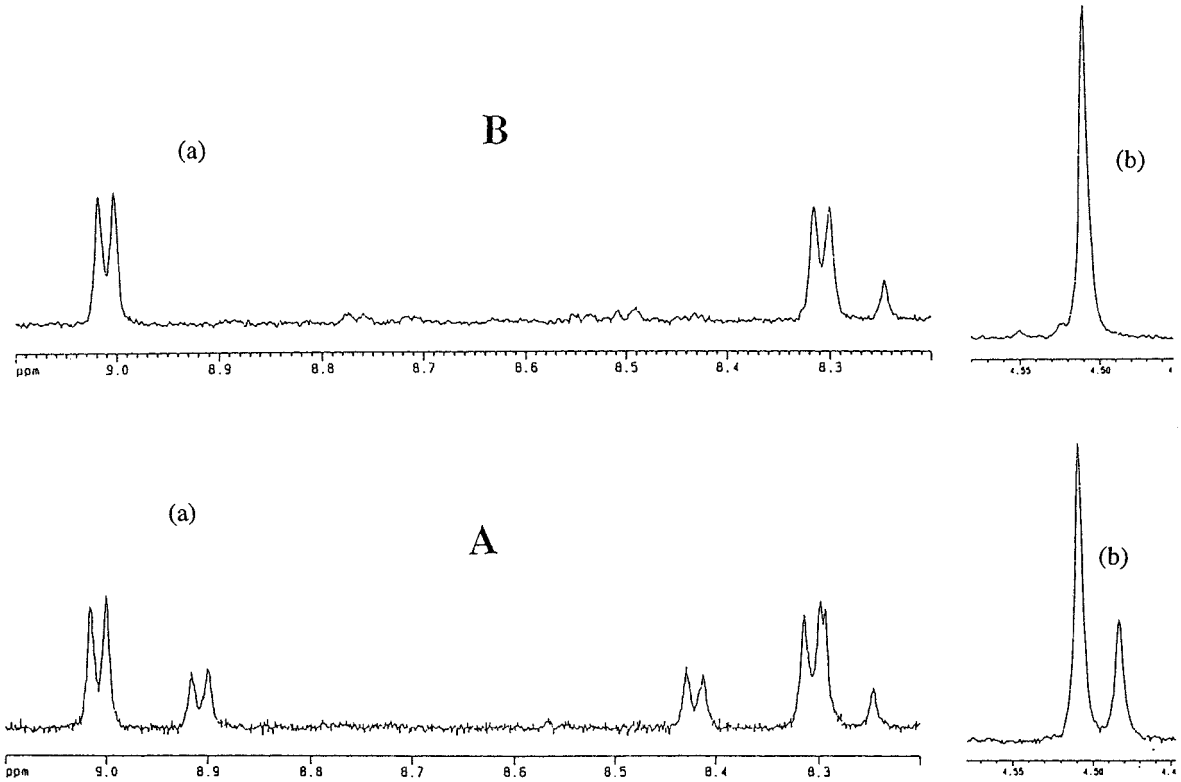

Figure 6. (A) ^{1}H NMR spectrum (DMF-d_7) of an immediately dissolved [DCF^{2-} · · ·*trans*-**1**] complex. (B) Spectrum after heating the sample for 90 min at 320 K.

system formed upon dissolution of the crystalline complex consists of a mixture of the non-symmetrical [(DCF^{2-}) · · ·*trans*-**1**/*trans*-**1**] complex and the symmetrical [DCF^{2-} · · ·*trans*-**1**] complex. Upon heating of the sample, the [(DCF^{2-})$_2$ · · ·*trans*-**1**/*trans*-**1**] complex is transformed to the symmetrical supramolecular assembly [DCF^{2-} · · ·*trans*-**1**]. These results are different and opposite to those observed for the supramolecular complexes between eosin and *N*,*N*′-dimethyl-4,4′-bipyridinium (MV^{2+}) in DMF. In this latter system the kinetic transformation from a 1:1 [eosin–MV^{2+}] to a mixed [(eosin)$_2$ · · · MV^{2+}:MV^{2+}] configuration was observed.[15]

The kinetics of this transformation can be followed spectroscopically. A low concentration of the crystalline [DCF^{2-} · · ·*trans*-**1**] complex can be solubilized in DMF without external heating. Figure 7 (curve a) shows the absorption spectrum of the solubilized complex. It reveals an absorption maximum at $\lambda = 517$ nm. Upon heating the sample (1 h, 40 °C) the system yields the spectrum shown in Figure 7 (curve b). The maximum absorption band increases in its intensity and is shifted by 5 nm to $\lambda = 512$ nm, and an additional absorption band at $\lambda = 611$ nm is observed. This spectral transformation is irreversible, and cooling of the sample does not influence the absorption spectrum. According to the ^{1}H NMR analysis, we attribute spectrum b in Figure 7 to the supramolecular complex [DCF^{2-} · · ·*trans*-**1**], where the initial spectrum (a) belongs to the complex [(DCF^{2-})$_2$ · · ·*trans*-**1**/*trans*-**1**]. By following the absor-

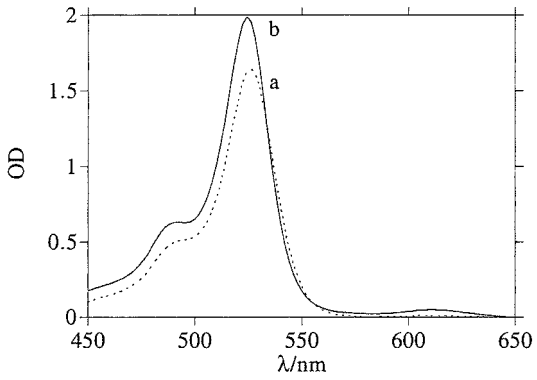

Figure 7. Absorption spectra of the complex between DCF^{2-} and *trans*-**1**: (a) immediately upon dissolution of the [DCF^{2-} · · ·*trans*-**1**] crystal complex in DMF; (b) after heating the sample for 1 h at 333 K.

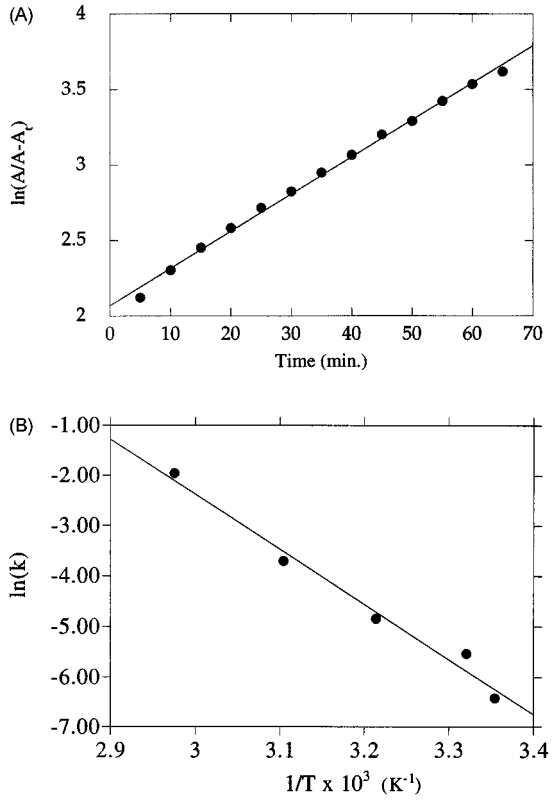

Figure 8. (A) First-order kinetic analysis of the absorbance changes at $\lambda = 540$ nm, corresponding to the transformation of the [(DCF^{2-})$_2$ · · ·*trans*-**1**/*trans*-**1**] complex to [DCF^{2-} · · ·*trans*-**1**] at 322 K. (B) Arrhenius plot for the first-order rate constants corresponding to the transformation of the [(DCF^{2-})$_2$ · · ·*trans*-**1**/*trans*-**1**] complex to the [DCF^{2-} . . . *trans*-**1**] supramolecular complex.

bance changes of the system at different temperatures, the kinetics of the transformation between the two supramolecular complexes [equation (6)] could be characterized. Figure 8(A) shows the kinetic analysis of the absorbance changes of the system at $\lambda = 540$ nm at 322 K. The derived rate constant corresponds to $k = 0{\cdot}22\ s^{-1}$.

$$[(DCF^{2-})_2 \cdots \textit{trans}\text{-}\mathbf{1}/\textit{trans}\text{-}\mathbf{1}] \xrightarrow{k} [(DCF^{2-}) \cdots \textit{trans}\text{-}\mathbf{1}] \quad (6)$$

Figure 8(B) shows the Arrhenius plot for the rate constants for this transformation at different temperatures. The derived activation energy corresponds to $E_a = 20$ kcal-mol^{-1}.

CONCLUSIONS

The study has revealed different affinities of *trans*- and *cis*-**1** to form donor–acceptor complexes with dichlorofluorescein [DCF^{2-} (**2**)]. The substantially lower affinity of *cis*-**1** to form the donor–acceptor complex with DCF^{2-} is attributed to the non-planar π-system of *cis*-**1** that originates from the *peri* repulsive interactions of H-atoms attached t the pyridinium rings linked to the ethylene bond. This structural distortion of the π-system prevents effective interlayered $\pi-\pi$ overlap between the donor and acceptor units. The supramolecular complexes between DCF^{2-} and *trans*-**1** were characterized in the solid state and in solution. In water and DMF, the primary kinetically stabilized [(DCF^{2-})$_2$ · · ·*trans*-**1**/*trans*-**1**] complex transforms to the thermodynamically stable, symmetrical, donor–acceptor complex [DCF^{2-} · · ·*trans*-**1**] [k (at 322 K) = $0{\cdot}22\ s^{-1}$, $E_a = 20$ kcal mol^{-1}].

REFERENCES

1. W. Saenger, *Principles of Nucleic Acid Structure*, pp. 132–140. Springer, New York (1984).
2. L. P. G. Wakelin, *Med. Res. Rev.* **6**, 275 (1986).
3. A.H.-J. Wang, G. Ughetto, G. J. Quigley and A. Rich, *Biochemistry* **26**, 1152 (1987).
4. (a) G. G. Desiraju and A. Gavezzotti, *J. Chem. Soc., Chem. Commun.* 621 (1989); (b) G. R. Desiraju (Ed.), *Organic Solid-State Chemistry.* Elsevier, Amsterdam (1987).
5. (a) B. Askew, P. Ballester, C. Buhr, K. S. Jeong, S. Jones, K. Paris, K. Williams and J. Rebek, *J. Am. Chem. Soc.* **111**, 1082 (1982); (b) J. Jazwinski, A. J. Blacker, J.-M. Lehn, M. Cesario, J. Guilhem and C. Pascard, *Tetrahedron Lett.* **28**, 6057 (1987); (c) J.-Y. Orthaland, A. M. Z. Slawin, N. Spencer, J. F. Stoddart and D. J. Williams, *Agnew. Chem., Int. Ed. Engl.* **1**, 1394 (1989).
6. (a) H.-J. Schneider, T. Blatter, S. Simova and I. Thesis, *J. Chem. Soc., Chem. Commun.* 580 (1989); (b) R. E. Sheridan and H. W. Whitlock, *J. Am. Chem. Soc.* **110**, 4071 (1988); (c) S. C. Zimmerman, M. Mrksich and M. J. Baloga, *J. Am. Chem. Soc.* **111**, 8528 (1989); (d) A. Mahammed, M. Rabinovitz, I. Willner, E. Vogel and M. Pohl, *J. Phys. Org. Chem.* **8**, 647 (1995).
7. D. Valdes-Aguilera and D. C. Neckers, *Acc. Chem. Res.* **22**, 171 (1989).
8. (a) W. R. Scheidt and Y. J. Lee, *Structure and Bonding*, Vol. 64. Springer, Berlin (1987).
9. C. A. Hunter, J. K. M. Sanders, *J. Am. Chem. Soc.* **112**, 5525 (1990).
10. (a) J. L. Lippert, M. W. Hanna, in *Molecular Complexes*, edited by R. Foster, Vol. 1. Eleck Science, London (1973); (b) C. J. Bender, *Chem. Soc. Rev.* **15**, 475 (1986).
11. P. Claverie, in *Intermolecular Interactions: from Diatomics to Biopolymers*, edited by B. Pullman, pp. 69–306. Wiley, Chichester (1978).
12. (a) J. Rebek, Jr and D. Nemeth, *J. Am. Chem. Soc.* **107**, 6738 (1985); (b) F. Diederich, *Angew. Chem., Int. Ed. Engl.* **27**, 362 (1988); (c) W. H. Pirkle and J. C. Pchaspkj, *J. Am. Chem. Soc.* **109**, 5975 (1987).
13. (a) D. B. Amabilino, P. R. Ashton, A. S. Reder, N. Spencer and J. F. Stoddart, *Angew. Chem., Int. Ed. Engl.* **33**, 433 (1994); (b) P. R. Ashton, C. L. Brown, E. J. T. Chrystal, T. T. Goodnow, A. E. Kaifer, K. P. Parry, A. M. Z. Slawin, N. Spencer, J. F. Stoddart and D. J. Williams, *Angew. Chem., Int. Ed. Engl.* **30**, 1039 (1991); (c) P. R. Ashton, R. Ballardini, V. Balzani, M. T. Gandolfi, D. J.-F. Marquis, L. Pérez-Garcia, L. Prodi, J. F.

Stoddart and M. Venturi, *J. Chem. Soc., Chem. Commun.* 177 (1994); (d) P. R. Ashton, A. S. Reder, N. Spencer and J. F. Stoddart, *J. Am. Chem. Soc.* **115**, 5286 (1993).
14. (a) P. L. Anelli, P. R. Ashton, N. Spencer, A. M. Z. Slawin, J. F. Stoddart and D. J. Williams, *Angew. Chem., Intl. Ed. Engl.* **30**, 1036 (1991); (b) P. Anelli, P. R. Ashton, R. Ballardini, V. Balzani, M. Delgado, M. T. Gandolfi, T. T. Goodnow, A. E. Kaifer, D. Philip, M. Pietaszkiewicz, L. Prodi, M. Reddington, A. M. Z. Slawin, N. Spencer, J. F. Stoddart and D. J. Williams, *J. Am. Chem. Soc.* **114**, 193 (1992).
15. I. Willner, Y. Eichen, M. Rabinovitz, R. Hoffman and S. Cohen, *J. Am. Chem. Soc.* **114**, 637 (1992).
16. I. Willner, Y. Eichen, A. Doron and S. Marx, *Isr. J. Chem.* **32**, 53 (1992).
17. I. Willner, S. Marx and Y. Eichen, *Angew. Chem., Int. Ed. Engl.* **31**, 1243 (1992).
18. S. Marx-Tibbon, I. Ben-Dov and I. Willner, *J. Am. Chem. Soc.* **118**, 4017 (1996).
19. G. M. Sheldrick, *Crystallographic Computing 3*, pp. 175–189. Oxford University Press, Oxford (1985).
20. D. G. Whitten, M. T. McCall, *J. Am. Chem. Soc.* **91**, 5097 (1969).

